SCIPEDIA

Improved Modal Parameter Identification of Spillway Radial Gate under Discharge Excitation based on COV-SSI

Yangliang Lu, Yakun Liu*, Ze Cao, Di Zhang and Chen Wang

School of Infrastructure Engineering, Dalian University of Technology, Dalian, 116024, China

INFORMATION

Keywords:
Spillway radial gate
discharge excitation
fluid-induced vibration
COV-ISSI
PHA clustering

DOI: 10.23967/j.rimni.2024.10.56527

Revista Internacional de Métodos Numéricos para Cálculo y Diseño en Ingeniería

Improved Modal Parameter Identification of Spillway Radial Gate under Discharge Excitation Based on COV-SSI

Yangliang Lu, Yakun Liu*, Ze Cao, Di Zhang and Chen Wang

School of Infrastructure Engineering, Dalian University of Technology, Dalian, 116024, China

ABSTRACT

This paper aims to improve the accuracy of modal parameter identification for Spillway Radial Gate (SRG) under discharge excitation. An Improved Covariance-driven Stochastic Subspace Identification (COV-ISSI) method, enhanced by Singular Entropy Increment (SEI) and Potential-based Hierarchical Agglomerative (PHA) clustering, is proposed. This method is designed to effectively eliminate false poles in the identification process. The performance of COV-ISSI is compared against the original stochastic subspace identification method, demonstrating its superior capability in accurately identifying modal parameters. Additionally, both the Additional Mass Method (AMM) and Direct Coupling Method (DCM) are employed to model the fluid-structure interaction system of the SRG. The derived vibration frequencies are compared with those obtained from COV-ISSI and an improved peak-picking method. Results show that the DCM closely aligns with COV-ISSI, with a relative error within 3%, while AMM results show significant deviation from the DCM. The proposed COV-ISSI method provides a reliable and automatic approach for identifying the operating frequencies of SRG structures, offering significant improvements over traditional methods.

OPEN ACCESS

Received: 24/07/2024

Accepted: 27/09/2024

Published: 07/04/2025

DOI
10.23967/j.rimni.2024.10.56527

Keywords:
Spillway radial gate
discharge excitation
fluid-induced vibration
COV-ISSI
PHA clustering

1 Introduction

The Spillway Radial Gate (SRG) is a critical facility for reservoir regulation and dam safety [1]. Sustainable hydropower generation requires the adjustable operation of the gate at small opening heights, which can lead to vibrations caused by the turbulence of high-speed water [2]. Fluid-induced Vibration (FIV) is the primary cause of dynamic instability in the supporting arms when the SRG is partially opened in dynamic water [3]. Notable examples include significant structural vibration damage to SRGs caused by discharge excitation, such as at Wachi Dam in Japan and Folsom Dam in the U.S. [4]. Significant research has been conducted on FIV in hydraulic gate structures [5–8]. To date, research on gate vibration can be categorized into four methods: principle analysis, hydroelastic model testing, prototype observation, and numerical simulation. For instance, Lee et al. [9] studied the Saemangeum tide embankment radial gate using the commercial computational fluid dynamics software ANSYS CFX. Additionally, Lian et al. [10] conducted comprehensive research on the severe

*Correspondence: Yakun Liu (liuyakun@dlut.edu.cn).

vibration of the SRG at Jinping Arch Dam in China during discharge operations, using prototype observation, numerical simulation, and theoretical derivation to explain the causes and mechanisms of the "accompanying" vibration phenomenon of the surface hole gate.

Operational Modal Analysis (OMA) for identifying modal parameters of hydraulic structures based on output responses under environmental excitation is gaining increasing popularity. In recent years, significant research on modal parameter identification for high dams has been conducted using the Stochastic Subspace Identification (SSI) method. For example, Li et al. [11] employed the Density-Based Spatial Clustering of Applications with Noise (DBSCAN) algorithm in conjunction with the Covariance-driven Stochastic Subspace Identification (COV-SSI) algorithm to identify the modal parameters of arch dam structures. Wang et al. [12] and Liu et al. [13] extracted modal parameters from vibration displacement data of an arch dam in southwest China under discharge excitation using the Data-driven Stochastic Subspace Identification (DATA-SSI) algorithm. Similarly, Mostafaei et al. [14] applied the DATA-SSI algorithm to identify the first four modes of the Koyna gravity dam during the Koyna earthquake.

There are two main methods for modal parameter identification of radial gates: the first is to conduct experimental modal analysis on standby gates when other gates are discharging, and the second is to perform OMA on gates during flood discharge. The first method can only obtain the dry modes of the gate and cannot capture the wet modes when the gate is partially open. Additionally, artificially exciting the gate in the first method makes it difficult to induce the overall modes of the gate, leading to high testing costs, long testing periods, and the potential for local structural damage. These limitations make traditional modal identification techniques challenging to apply in real-time health monitoring of radial gates. To date, there are few researches on the health monitoring of vibratory gate during actual operation, especially the modal parameter analysis of vibratory gate based on real-time vibration data. Based on a gate model with a geometric scale of 1:10 and COV-SSI method, Zhang et al. [15] analyzed the dynamic response of the radial gate. However, the gate model adopts a steel structure, which leads to over-high stiffness of the structure. Hence, the measured natural frequency is much higher than the actual steel gate, and the identified frequency differs significantly from the actual operation results of the gate. Hu et al. [16] identified the modal parameters of the radial gate through prototype observation based on COV-SSI and adopted pulse excitation method to collect the response data of the main components of the gate. Unfortunately, owing to the influence of water noise and white noise, the stabilization diagram of the gate contains a large number of false poles, which is difficult to achieve automatic intelligent identification. Cai et al. [17] employed the natural excitation technology alongside the eigensystem realization algorithm to identify the dynamic properties of a gate. However, due to the harsh environmental noise during the partial opening of the radial gate for flood discharge, the vibration signals collected by sensors contain a significant amount of noise, leading to inaccuracies in modal identification results. Efficient and precise noise reduction, as well as the elimination of false modes, is crucial for improving the dynamic monitoring of the operating modal parameters of radial gates.

In summary, the large size of gate structures, significant influence of strong field noise, and low signal-to-noise ratio of measured data present significant challenges for achieving rapid modal recognition of gate modes. In this study, the measured acceleration responses of the gate under discharge excitation are first denoised using a combination of Empirical Mode Decomposition (EMD), Multi-scale Permutation Entropy (MPE), and Wavelet Threshold Denoising (WTD). Next, the system order is determined using Singular Entropy Increment (SEI) for automatic order determination. Based on this, a Potential-based Hierarchical Agglomerative (PHA) method is employed to eliminate false poles

in the stabilization diagram. Finally, the numerically derived results from finite element method (FEM) simulations are compared to further validate the effectiveness of the PHA clustering method.

2 Methodology

2.1 COV-SSI Method

There are several algorithm variants of SSI, with two common ones being COV-SSI and DATA-SSI. The COV-SSI variant is simpler and easier to implement, and the resulting system description is deterministically balanced, making it theoretically optimal.

In practical engineering applications, measurement noise is inevitable. As a result, the discrete-time state equation for structures with n degrees of freedom subjected to white noise environmental excitation is:

$$\boldsymbol{x}_{k+1} = \boldsymbol{A}\boldsymbol{x}_{\boldsymbol{k}} + \boldsymbol{w}_k \tag{1}$$

$$\boldsymbol{y}_{k+1} = \boldsymbol{B}\boldsymbol{x}_{\boldsymbol{k}} + \boldsymbol{v}_k \tag{2}$$

where $\boldsymbol{x}_{\boldsymbol{k}}$ represents the value of the system state vector x at time k, and $\boldsymbol{y}_{\boldsymbol{k}}$ represents the value of the system output vector y at time k; $\mathbf{A}$ is the system state matrix, $\boldsymbol{B}$ is the system output matrix, $\boldsymbol{w}_k$ is the noise caused by process and modeling errors; $\boldsymbol{v}_k$ represents the noise caused by sensor errors.

By defining the Hankel matrix and constructing the Toeplitz matrix from the covariance of the output response data, singular value decomposition is applied to derive the system state matrix $\boldsymbol{A}$ and the output matrix $\boldsymbol{B}$, followed by eigenvalue decomposition on the discrete state matrix $\boldsymbol{A}$:

$$\mathbf{\Lambda} = \mathbf{\Psi}\mathbf{\Lambda}\mathbf{\Psi}^{-1} \tag{3}$$

where $\mathbf{\Lambda} = diag[\mu_i]$ is a diagonal matrix composed of discrete complex eigenvalues, and $\mathbf{\Psi}$ is the matrix consisting of the system's eigenvectors.

Let λ_i represent the i-th continuous-time eigenvalue, μ_i denote the discrete system eigenvalue, and Δt indicate the sampling interval. To extract the modal parameters from the system matrix identified by the stochastic subspace method, it is only necessary to separate the eigenvalues and eigenvectors of the state equation from the obtained system matrix. The relationship of the eigenvalues for the discrete state-space equation of the structure is as follows:

$$\lambda_i = \frac{\ln \mu_i}{\Delta t} \tag{4}$$

The relationship between the system's complex eigenvalues, natural frequency, and damping ratio is as follows:

$$\lambda_i, \lambda_i^* = -\zeta_i\omega_i \pm j\omega_i\sqrt{1-\zeta_i^2} \tag{5}$$

where λ_i and λ_i^* are conjugates of each other, ω_i represents the system's natural frequency, and ζ_i represents the damping ratio.

Based on Formula (5), the system's natural frequency ω_i, damping ratio ζ_i, and mode shape $\mathbf{\Phi}_i$ can be obtained as follows:

$$w_i = \frac{\sqrt{(\lambda_i^*)^2}}{2\pi} \tag{6}$$

$$\zeta_i = \frac{\lambda_i + \lambda_i^*}{2\sqrt{\lambda_i \lambda_i^*}} \tag{7}$$

$$\boldsymbol{\Phi}_i = \boldsymbol{B}\boldsymbol{\Psi}_i \tag{8}$$

2.2 System Order Determination Based on SEI

When the input excitations are not known, the structural system's order is also undetermined, which plays a critical role in identifying modal parameters. Following the Singular Value Decomposition (SVD) of the system matrix, the resulting singular spectrum from the diagonal matrix can be expressed as follows:

$$\sigma_i = \log\left(q_i / \sum_{i=1}^{l} q\right) (i \leq 1) \tag{9}$$

where q_i represents the non-negative diagonal elements of the diagonal matrix, l represents the total count of non-zero singular values derived from the state matrix.

The singular spectrum represents the relative distribution of energy among different state variables within the entire system [13]. The concept of singular entropy is introduced to analyze how signal information changes with the order of the singular spectrum, and its calculation formula is:

$$E_r = \sum_{i=1}^{k} \Delta E_i \quad (k \leq 1) \tag{10}$$

where k represents the order of the singular entropy, and ΔE_i denotes the SEI at order i. The calculation follows the equation provided below:

$$\Delta E_i = -(q_i / \sum_{i=1}^{l} q) \log (q_i / \sum_{i=1}^{l} q) \ (i \leq 1) \tag{11}$$

For a vibration signal, when the finite characteristic information content reaches saturation, the SEI begins to decrease to an asymptotic value. Based on this, the SEI can be used to determine the order of a system. When the SEI reaches stability, the associated singular spectrum order can serve as an estimate for the system's order. After eliminating the non-modal components and conjugate pairs, the true order of the system is approximately $i/2$ [18].

2.3 PHA Clustering Method

In SSI for large-scale engineering structures, hierarchical clustering and non-hierarchical clustering are the dominantly adopted methods of the false pole elimination in the automatic identification of modal parameters. Their disadvantages include the need to set the initial clustering center in advance and the high complexity of the algorithm. Hierarchical clustering method is computationally expensive. Whereas the PHA clustering method overcomes the defect that non-hierarchical clustering has great dependence on the initial cluster center. The PHA clustering method has the advantages of fast and anti-noise.

In the physical sense of Newtonian gravitation, the gravitational force between point i and point j is:

$$\vec{F}_{ij}(\vec{r}_{ij}) = G\left(\frac{\hat{r}_{ij}}{r_{ij}^2}\right) \tag{12}$$

where $\vec{r}_{ij}$ denotes the vector from point i to point j; r_{ij} denotes the Euclidean distance between point i and point j; $\hat{r}_{ij}$ denotes the unit vector of $\vec{r}_{ij}$; G is the gravitational constant.

If the distance between the two points falls below the threshold δ, the gravitational force between them becomes zero, as described by the following equation:

$$MinD_i = \min_{r_{ij}\neq 0, j=1,2,\ldots,N}(r_{ij}) \tag{13}$$

$$\delta = mean(MinD_i)/S \tag{14}$$

where $MinD_i$ represent the shortest distance from point i to any other point; and S is a scaling factor, generally set to 10 [19]. Then we define the potential at point i from point j as:

$$\Gamma_{ij}(r_{ij}) = \int_{r_{ij}}^{\infty} \underset{F_{ij}}{\rightarrow}(\underset{r}{\rightarrow}) \cdot \hat{r}dr = \begin{cases} -G\dfrac{1}{r_{ij}}, & r_{ij} < 0 \\ -G\dfrac{1}{\delta}, & r_{ij} \geq 0 \end{cases} \tag{15}$$

When G is 1, the potential energy Γ_i of each point can be obtained from Formula (16):

$$\Gamma_i = \sum\nolimits_{j=1,2,\ldots,N} \Gamma_{ij}(r_{ij}) \tag{16}$$

By using Parzen window method for non-parametric probability density estimation, the relationship between total potential energy and probability density distribution is as follows:

$$\Gamma_i = (-N/\alpha)\hat{p}_N(i) \tag{17}$$

where α is the normalization constant ensuring the window function integrates to 1 across the entire feature space, and $\hat{p}_N(i)$ is probability density function of data point in a new window function.

2.4 The Clustering Steps

The main steps of modal clustering judgment are as follows:

Step 1: The distance between each modal point serves as the clustering criterion, with the modal distance formula d_{i-j} established by Magalhães et al. [20], which considers frequency and mode characteristics, is adopted in this paper.

$$d_{i-j} = \left|\frac{f_i - f_j}{f_i}\right| + 1 - MAC(\Phi_i, \Phi_j) \tag{18}$$

where f_i, f_j represent the natural frequencies of the i-th and j-th modes calculated by COV-SSI algorithm, respectively; Φ_i and Φ_j respectively represent the mode shapes of the i-th and j-th modes. MAC denotes the modal assurance criterion, that can be calculated as follows:

$$MAC(\Phi_i, \Phi_j) = \frac{(\Phi_i^T \Phi_j)^2}{(\Phi_i^T \Phi_j)(\Phi_j^T \Phi_i)} \tag{19}$$

Subsequently, the modal distance matrix d_i is derived by computing the distances between each pair of data points.

Step 2: According to the obtained d_i, calculate the potential energy of each point Γ_i using Formulas (14)~(17). The modal distance matrix d_i is obtained by calculating the modal distance d_{i-j} between all the data points.

Step 3: All the data points are ranked successively by their potential value, and the parent point of each sample is determined according to the parent point definition (20) and d_i.

$$parent[i] = arg\,\underset{k}{min}(r_{k,i}|\Gamma_k \leq \Gamma_i, k \neq i) \tag{20}$$

where k represents data points that excludes the point i. Here, the data points correspond to the potential energy values Γ_k calculated according to Formulas (18)∼(20).

Step 4: Calculate the distance between the data point and its parent point, then build the edge-weighted tree, where the root node is the point with the minimum potential value.

Step 5: According to the given distance threshold d_{max}, the hierarchical clustering algorithm is applied to derive the final clustering outcome.

3 Modal Identification of a Six-Degree-of-Freedom (6-DOF) System

3.1 Construction of 6-DOF Shear Model

To validate the program's efficiency, a 6-DOF system is initially designed, as shown in Fig. 1.

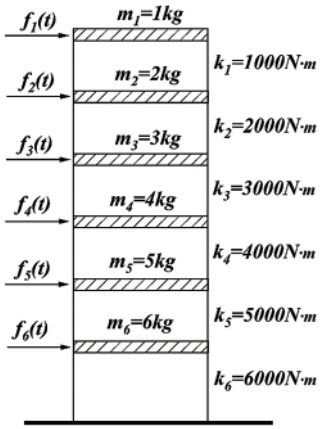

Figure 1: Six-layer shear model

Then the mass and stiffness matrices of the system can be obtained as follows:

$$\mathrm{M} = \begin{vmatrix} 1 & 0 & 0 & 0 & 0 & 0 \\ 0 & 2 & 0 & 0 & 0 & 0 \\ 0 & 0 & 3 & 0 & 0 & 0 \\ 0 & 0 & 0 & 4 & 0 & 0 \\ 0 & 0 & 0 & 0 & 5 & 0 \\ 0 & 0 & 0 & 0 & 0 & 6 \end{vmatrix} \tag{21}$$

$$\mathrm{K} = \begin{vmatrix} 1 & -1 & 0 & 0 & 0 & 0 \\ -1 & 3 & -2 & 0 & 0 & 0 \\ 0 & -2 & 5 & -3 & 0 & 0 \\ 0 & 0 & -3 & 7 & -4 & 0 \\ 0 & 0 & 0 & -4 & 9 & -5 \\ 0 & 0 & 0 & 0 & -5 & 11 \end{vmatrix} \times 1000 \tag{22}$$

Suppose that the damping matrix of the structure satisfies the linear combination of stiffness matrix and mass matrix, the Rayleigh damping matrix is set as follows:

$$C = 0.2 \times \mathrm{M} + 0.003 \times \mathrm{K} \tag{23}$$

Firstly, the Gaussian white noise excitation with a sampling frequency of 100 Hz and a time length of 100 s is constructed, resulting in totally 10,000 data points generated. Secondly, the structural response at each DOF is calculated using the Newmark−β method. To simulate measured acquisition noise, we add 20% Gaussian white noise to the acceleration data of each channel. Finally, the acceleration responses containing 20% Gaussian white noise are taken as input of the system and substituted into COV-ISSI. The block row number i of the Hankel matrix is set to 30. It is assumed that the minimum order value of the dynamic system is 1, the maximum value is 50.

3.2 Automatic Modal Parameter Identification Based on the PHA Algorithm

3.2.1 System Order Determination using SEI

Fig. 2 shows the magnitude of the signal SEI values at different system orders. According to complex mode theory [21] that the real order of the system is half of the system order, the final actual order of the system is 12/2 = 6, which accords with the 6-DOF system in the example.

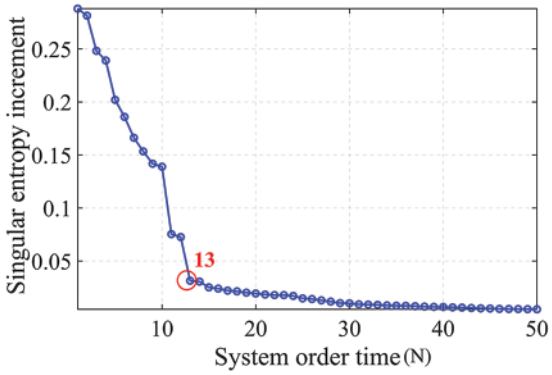

Figure 2: SEI at different orders of the system

3.2.2 Numerical Simulation Results and Analysis

When COV-SSI is adopted to identify the modes, it is very difficult to analyze the stability diagram due to the existence of false poles. Therefore, the stable poles are initially determined by setting the errors of frequency, damping ratio and mode shapes as 1%, 5% and 2% [22], respectively. Secondly, the false poles are further eliminated by PHA clustering. Table 1 lists the identified and simulated natural frequencies. The identified results agree well with the simulated values with maximum percentage deviation of less than 3%. The stabilization diagram of the 6-DOF system identified by COV-SSI is shown in Fig. 3. It can be observed from Fig. 3a that many points with frequencies deviate from the theoretical values yet satisfying the stability requirements exists, which are all removed after PHA clustering as is presented in Fig. 3b.

Table 1: Comparison between identification value and calculated value of 6-DOF system

Modal order	Identification value (Hz)	Theoretical value (Hz)	Relative error (%)
First-order	1.650	1.638	0.732
Second-order	3.544	3.592	1.336
Third-order	5.370	5.372	0.037
Fourth-order	6.854	6.913	0.853
Fifth-order	7.991	8.166	2.143
Sixth-order	8.987	9.109	1.339

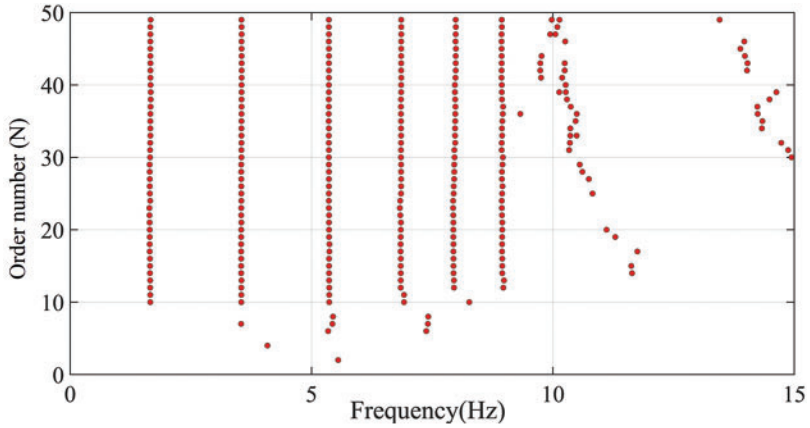

(a) Stabilization diagram without PHA clustering

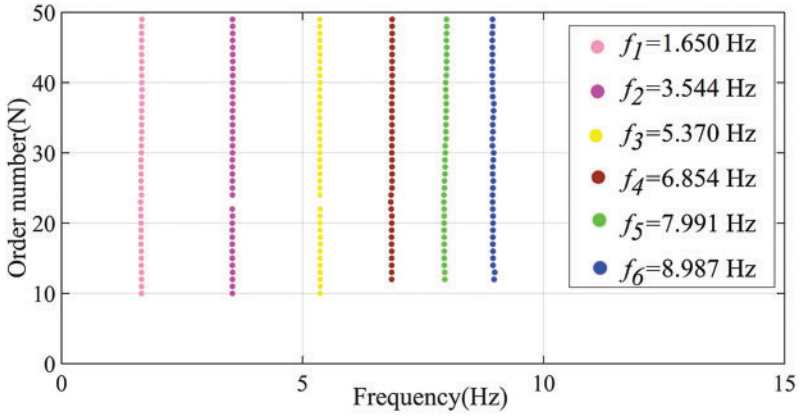

(b) Improved stabilization diagram after PHA clustering

Figure 3: Stabilization diagram of 6-DOF

Fig. 3b shows the stabilization diagram of PHA clustering after screened out false poles. It can be found from the diagram that the real stable poles are perfectly retained. The mode shapes calculated according to the automatic recognition program are shown in Fig. 4 that agree perfectly with the true values. Fig. 5 shows the three-dimensional histogram of MAC identified from the proposed method. All diagonal values are close to 1, and all non-diagonal values are close to 0. The results of MAC

values show that the mode identified by the proposed method presents good consistency with the theory. It indicates that the intelligent algorithm adopted in this paper can accurately obtain the modal parameters of the 6-dof mass-spring-damping system, all the false poles are eliminated, and the stability diagram is very neat, which will bring great convenience in the following analysis.

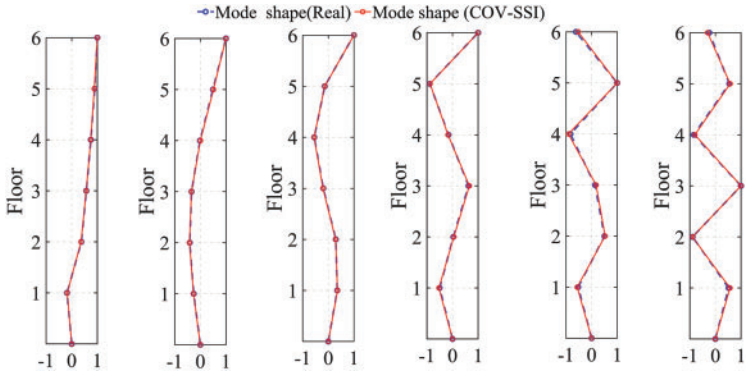

Figure 4: Mode shapes comparison between theoretical and recognized modes

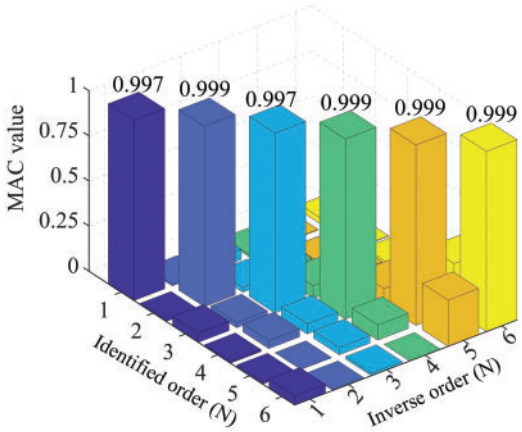

Figure 5: MAC value

4 Modal Parameter Identification of SRG

4.1 Engineering Introduction and Layout of Measuring Sensors

To verify the effectiveness of the improved algorithm for SRG modal parameter identification, data were collected from a SRG of a gravity dam located in Yalong River, in China. The maximum height of the dam is 168 m. The spillway section is arranged with 5 SRGs, each SRG with the width of 15.00 m and the radius of 21.00 m. The discharge flow pattern of the gate is presented in Fig. 6a, b. To comprehensively monitor the vibration characteristics in the sensitive areas (main beam and supporting arm) under hydrodynamic loads, three triaxial acceleration sensors, developed by the China Orient Institute of Noise & Vibration, were deployed on the top-left arm of SRG (sensor No. 3#) to capture axial, vertical, and lateral vibrations. Additionally, two triaxial acceleration sensors were installed on the upper and lower main beam of the gate. The placement of these sensors is illustrated in Fig. 7. The triaxial acceleration sensors possess a sensitivity of 1000 mV/g, with a frequency range

between 0.1 and 2 kHz and a resolution of 0.00002 g. Each gate opening was sampled at a frequency of 200 Hz, with a duration of 120 s. Distributions of seven measuring points are shown in Fig. 7 numbered as A1–A7. In this study, vibration acceleration data under operating conditions of the gate opening height 3.5 m is selected to identify the modal parameters. The upstream water level is 1328.98 m, and the corresponding water height in front of the gate is 11.42 m.

Figure 6: Flow pattern of 3# spillway gate opening

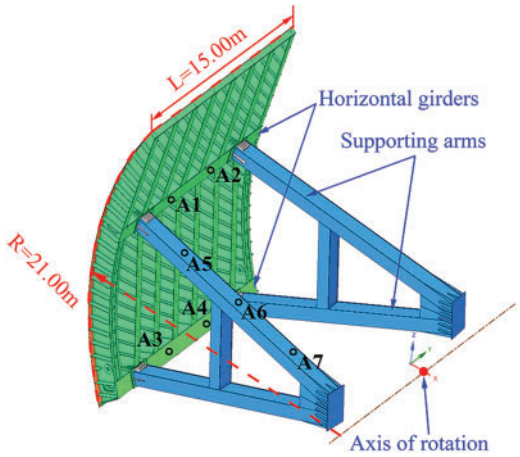

Figure 7: Locations of gate acceleration sensor installation

4.2 Improved Modal Parameter Identification Results

The flow chart of improved modal parameter identification algorithm of SRG is presented in Fig. 8.

4.2.1 Noise Reduction Processing

The acceleration vibration response of the SRG is a nonlinear signal with a low signal-to-noise ratio, indicating that its valuable information is masked by low-frequency water flow disturbances and high-frequency background noise [23]. In this work, the EMD-MPE-WTD method is used to filter out background noise. The WTD method is particularly effective at suppressing high-frequency

white noise. A soft threshold function is employed to address the issue of discontinuity present in hard threshold functions, resulting in improved continuity and more accurate denoising outcomes.

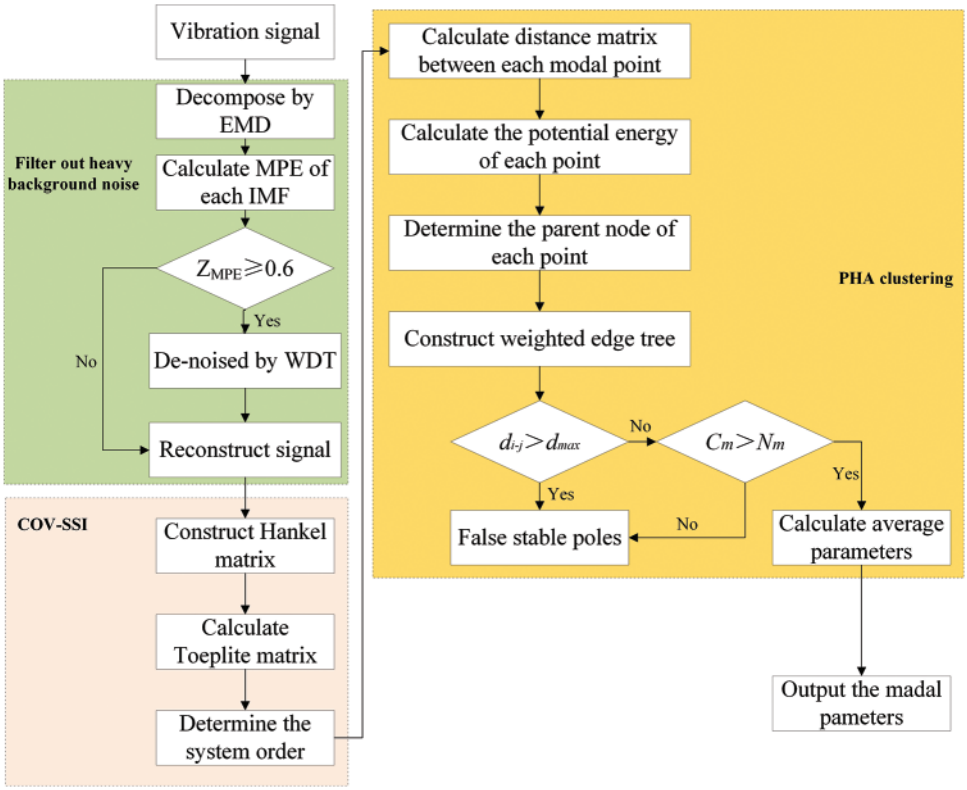

Figure 8: Improved modal parameter identification algorithm of SRG

4.2.2 Identification Result Analysis Based on COV-ISSI

The Hankel matrix is constructed after the signal is de-noised. Then the COV-ISSI is adopted to obtain the variation of SEI with the order of singular spectrum in the intact state, as shown in Fig. 9. When the order reaches about the 7, the decreasing rate of SEI is much slowed down. At this stage, the available signal feature information reaches a saturation point, indicating that most of the relevant characteristics have been captured and the information is essentially comprehensive. The final actual vibration order of the gate system is 3 after removing the non-modal and conjugate terms from the eigenvalues.

The stabilization diagram's maximum order was defined as 100, with frequency, damping ratio, and mode shape tolerances established at 0.02, 0.1, and 0.01, respectively. Then the stabilization diagram before noise reduction is obtained, as shown in Fig. 10a. It can be observed that besides the true stable poles, many false poles are identified due to the existence of noise. After de-noised using WTD, as is shown in Fig. 10b, it can be clearly seen that the relatively high-frequency noise is filtered out and some discrete false poles in the low frequency region are also eliminated. However, non-negligible false poles still exist in the stabilization diagram, which will undoubtedly interfere the effectiveness of modal parameter identification. Therefore, PHA clustering is implemented with the results plotted in Fig. 10c. Three frequencies, 7.997, 11.661 and 13.404 Hz can be observed that are clearly identified.

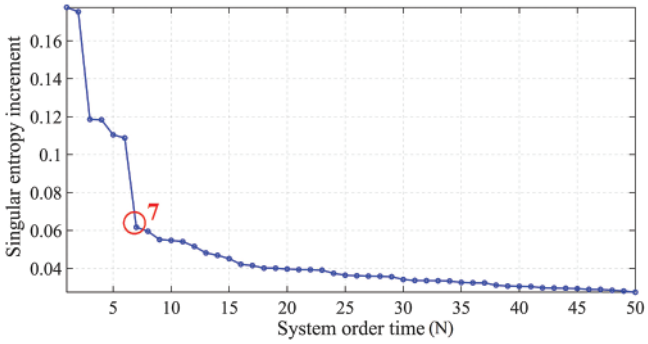

Figure 9: Trend of SEI

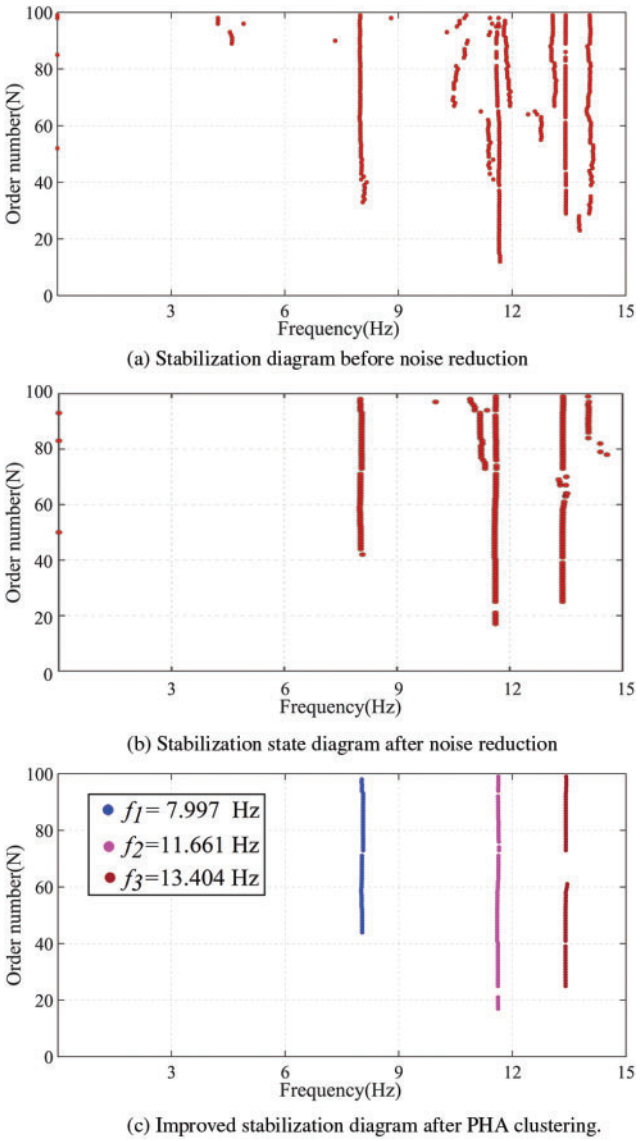

Figure 10: Stabilization diagram of SRG

4.3 Improved Peak-Picking (IPP) Method

In practical engineering, the peak-picking method is a commonly employed approach for identifying modal parameters. However, since a single sensor signal only captures local characteristics of the structure, it is susceptible to interference from environmental background noise. To tackle this problem, this paper introduces a method for fusing information by integrating vibration. This approach aims to enhance the extraction of dynamic information from the SRG by leveraging data from various locations.

4.3.1 Correlation Variance Dedication Rate Algorithm

Data-level fusion is based on the collected original data, by fusing the calculated data of the measured multi-channel signal. This method can effectively eliminate the uncertainty of data derived from isolated sensor. In the literature [24], a method of data-level fusion based on the correlation function between vibration signals is proposed, which has good anti-interference performance. Additionally, Zhang et al. [25] introduced a data-level fusion approach for multi-sensor dam body vibration response, utilizing the Variance Dedication Rate (VDR). In comparison to the fusion method based on the correlation function, this method can effectively extract the dense frequency information and has good universality by introducing dynamic fusion coefficient. Combining the correlation function and VDR, in this paper we adopt a data-fusion algorithm named as Correlation Variance Dedication Rate (CVDR), and its fusion process is shown in Fig. 11.

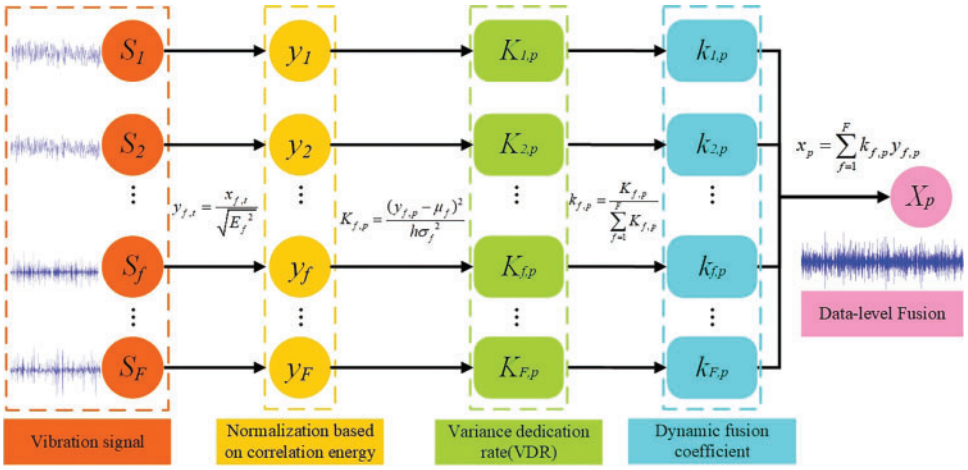

Figure 11: Dynamic data-level fusion based on CVDR

4.3.2 Modal Parameter Identification of SRG Based on IPP

The acceleration time series from measuring point A1 on the upper main beam and points A6 and A7 on the supporting arm were selected for data-level fusion. Fig. 12 presents the dynamic fusion coefficient curves, while Fig. 13a shows the fused time history curve, and Fig. 13b displays the corresponding normalized power spectrum curve. The derived first 3 frequencies, 8.001, 11.572 and 13.428 Hz agree well with the results of COV-SSI. However, a fourth peak at approximately 9.131 Hz indicates the uncertainty in the implementation.

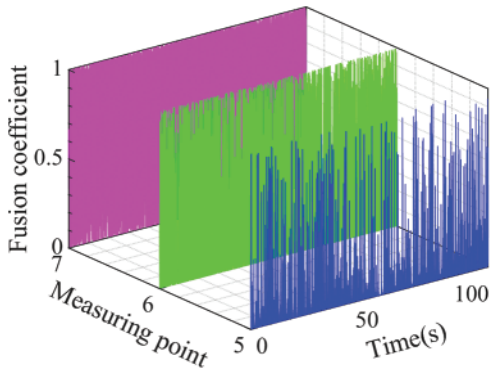

Figure 12: Dynamic fusion coefficient curves of gate vibration responses

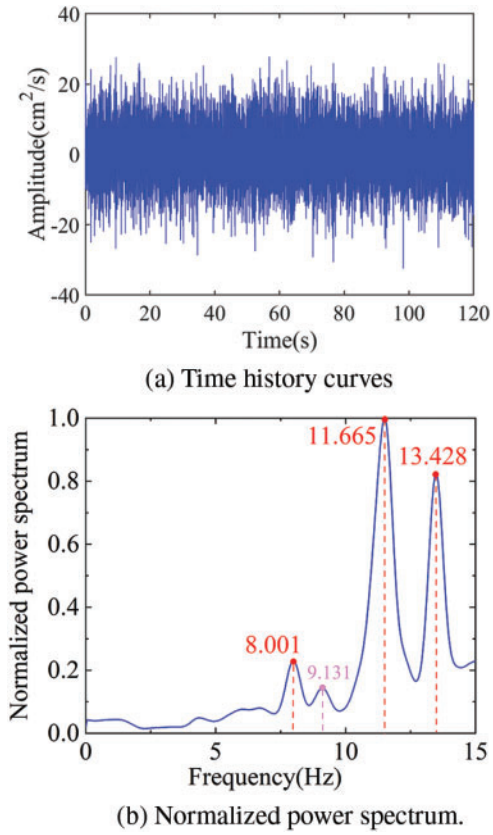

Figure 13: Dynamic fusion coefficient of gate vibration responses

4.4 FEM of SRG

In order to verify the feasibility and accuracy of this work, the results of the COV-ISSI identification are compared with the modal parameters obtained by the finite element calculation of the SRG. The dynamic characteristics of the SRG under discharge excitation are essentially the Fluid-Structure Interaction (FSI) problem of the interaction between water body and steel gate. According to the principle of Additional Mass Method (AMM) and Direct Coupling Method (DCM), two kinds

of three-dimensional FEM of the gate structure with different coupling forms are established. The schematic diagram is shown in Fig. 14. Assuming that the water body is non-viscous, compressible and has small disturbance, and the solid is linearly elastic, a 3D FEM model of SRG and water body is established using the finite element theory of FSI system. All the components of the gate structure, including the panel, main beam, horizontal sub-beam, vertical sub-beam, bottom beam, side beam and supporting arm are modeled using shell elements. The shell181 element in finite element software ANSYS is selected to establish SRG structure [26], which can reflect the combined deformation of the components such as bending, torsion and shear, and retain the main characteristics of SRG structure. The water coupling effect of the AMM is realized by adding mass21 elements to the area where the gate panel touches the water body, whereas DCM adopts fluid30 three-dimensional acoustic fluid element simulation, and set the interface between the gate panel and the water body as the fluid-structure coupling interface during coupling calculation. Consequently, the element nodes on the coupling surface share the same displacement and pressure, with the length of the water body set to five times the height of the gate's water body. The FSI model of DCM has a total of 68,913 structural elements and 238,650 fluid elements. Model parameter selection of steel and water body is listed in Table 2.

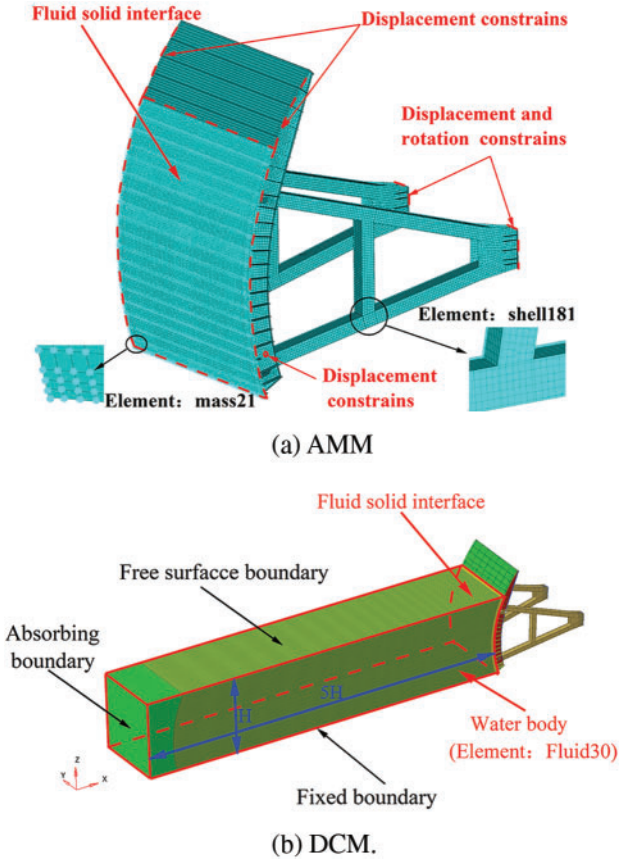

Figure 14: Two different gate-water coupling models

Table 2: Model parameter selection of steel gate and waterbody

Steel material		Water body	
Element type	Shell181	Element type	Fluid30
Density	7850 kg/m^3	Density	1000 kg/m^3
Elastic modulus	206 GPa	Speed of sound	1440 m/s
Poisson ratio	0.3	/	

Boundary Conditions Setup: When the opening height of the SRG is 3.5 m, the vertical flow direction of the side beam is directly restricted to replicate the impact of the side pier's constraints on the gate. Additionally, a local coordinate system is established at the lifting lug of the opening and closing rod to allow rotational freedom. At the hinges, translational displacement is restricted, while only rotational angular displacement around the hinges is permitted relaxed.

4.5 Results and Discussions

The wet modes and dry modes of the two coupling models are analyzed using ANSYS APDL. The first three frequencies of the gate structure are listed in Table 3 and the mode shapes are plotted in Fig. 15. According to the identification results of FEM and COV-ISSI, it is shown that: The errors between the gate natural vibration frequency using the DCM and the COV-ISSI identification results are between 1.164% and 2.032%. However, the frequency calculated by the AMM is significantly smaller than the gate natural vibration frequency under the fluid-structure coupling. Although the modal patterns calculated by the AMM are similar to those obtained by the DCM, the identified frequencies are significantly different from those obtained by the DCM and modal parameter identification. Hence, the coupling model of AMM cannot fully reflect the inherent characteristics of the SRG. The AMM is an approximate formula for solving the pressure at the working surface of the Westergaard rigid dam. It is only a simple linear fluid-structure coupling model, which is transformed into the action form of water body and neglects the compressibility of water body [27]. It is worth noting that Cai et al. [17] collected the measured dynamic displacement of the deep hole gate of the Three Gorges Project and used Next-ERA to identify the modal parameters of the radial gate. However, the finite element analysis results ignored the contact boundary conditions of the gate and the influence of the water body, and the FEM results of the gate are not convincing.

Table 3: Comparison of recognition frequencies of SRG

Modal order	Frequency (Hz)				Difference among COV-ISSI, FEM and IPP (%)		
	DCM	AMM	COV-ISSI	IPP	COV-ISSI	IPP	AMM
First-order	7.905	5.195	7.997	8.001	1.164	1.290	34.282
Second-order	11.526	7.026	11.661	11.665	1.171	1.206	39.042
Third-order	13.137	7.826	13.404	13.428	2.032	2.215	40.428

It can be observed from Fig. 15 that the gate vibration patterns of FEM show that the low-order vibration patterns of the gate leaf are mainly the bending deformation of the upper cantilever structure and the bulging deformation of the middle of the gate leaf, and the torsional vibration

and tangential deformation vibration of the supporting arms. The FEM results of the gate vibration pattern mentioned above are close to those of the gate calculated by Lian et al. [10].

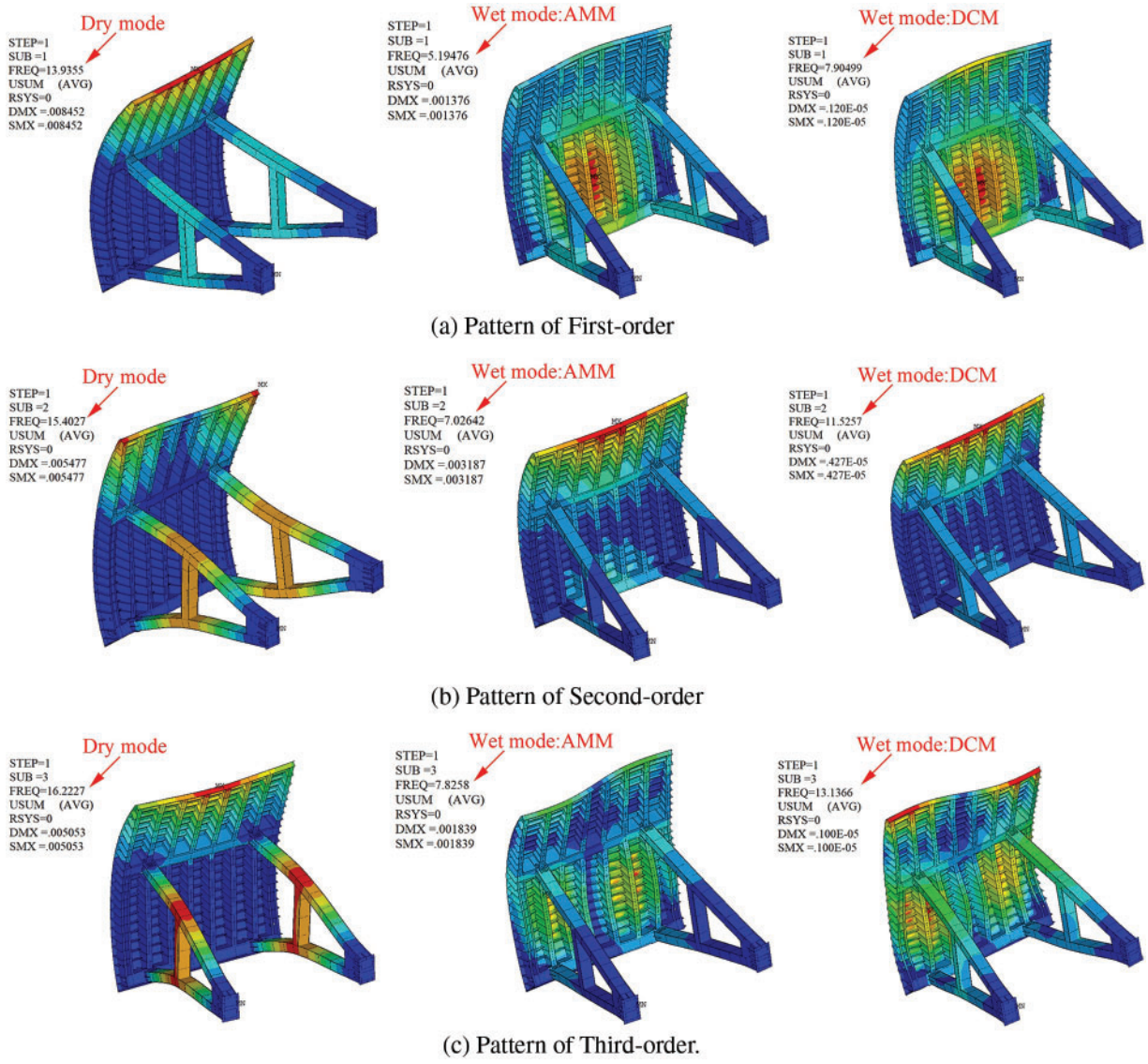

Figure 15: Gate vibration patterns of FEM

The results of FEM and COV-ISSI confirm each other, indicating that the mode identification method based on COV-ISSI has the ability to extract the modal parameters of the SRG under discharge excitation.

5 Conclusions

Based on the COV-ISSI, IPP, and FEM calculation results for the SRG, the following conclusions can be drawn:

1. The accuracy of the COV-ISSI algorithm based on the SEI and PHA clustering is validated using a 6-DOF shear model.

2. The natural vibration frequency of the gate in its dry mode is higher than when influenced by the water body. The AMM results significantly differ from those obtained using IPP and DCM, failing to capture the coupling effect between the water body and the gate structure. In contrast, the natural vibration frequency results from DCM, calculated using FEM, align well with the COV-ISSI identification, offering a more accurate representation of the gate structure's natural vibration characteristics. The maximum relative error between the frequency identification results and the FEM values is less than 3%, which meets engineering accuracy requirements.

3. The IPP method has the drawback of subjectively selecting peaks. In contrast, the COV-ISSI method, based on SEI and PHA, can efficiently, automatically, and accurately identify the modal parameters of the SRG. This improved method is capable of quickly identifying the real-time online modal parameters of the SRG under discharge excitation.

Accurately improving the damping ratio of SRG is a critical issue that needs to be addressed in future research. Additionally, it is essential to develop methods for precisely identifying the complex mode shapes of SRG using a limited number of acceleration sensors through OMA method.

Acknowledgement: None.

Funding Statement: This research was supported financially by the National Natural Science Foundation of China (Grant Nos. 52179060 and 52479060).

Author Contributions: Study conception and design: Yangliang Lu, Yakun Liu and Ze Cao; data collection:Yangliang Lu, Yakun Liu and Ze Cao; analysis and interpretation of results: Yangliang Lu, Yakun Liu and Di Zhang; draft manuscript preparation: Yangliang Lu and Chen Wang. funding acquisition, Yakun Liu and Di Zhang. All authors reviewed the results and approved the final version of the manuscript.

Availability of Data and Materials: Data cannot be made publicly available; readers should contact the corresponding author for details.

Ethics Approval: Not applicable.

Conflicts of Interest: The authors declare no conflicts of interest to report regarding the present study.

References

1. Shi SJ, Han YF, Hu KJ, Zhou YD, Hu TY, Lou YD, et al. Study on dynamic response characteristics of radial steel gate under rare earthquake considering fluid structure coupling effect. Revista Internacional De Métodos Numéricos Para Cálculo Y Diseño En Ingeniería. 2023 Apr;39(2):1–15. doi:10.23967/j.rimni.2023.04.004.
2. Xu C, Liu JL, Zhao CL, Liu F, Wang ZZ. Dynamic failures of water controlling SRGs of hydropower plants: advancements and future perspectives. Eng Fail Anal. 2023 Mar;148(1):1–18. doi:10.1016/j.engfailanal.2023.107168.
3. Liu YK, Ni HG, Ye ZQ, Liu YL. Analysis of flow-induced vibration of hydraulic radial gate. J Dalian Univ Technol. 2005 May;5:730–4 (In Chinese) doi:10.3321/j.issn:1000-8608.2005.05.021.

4. Anami K, Ishii N. Flow-induced dynamic instability closely related to Folsom Dam Tainter-Gate failure in California. In: 7th International Conference Flow-Induced Vibration (FIV 2000), 2000 Oct 5–8; Luzern, Switzerland.
5. Thang ND, Naudascher E. Vortex-excited vibrations of underflow gates. J Hydraul Res. 1986 Jan;24(2):133–51. doi:10.1080/00221688609499327.
6. Anami K, Ishii N, Knisely CW, Tsuji T, Oku T. Friction-maintained dynamic stability. In: 10th Biennial International Conference on Vibration Problems (ICOVP), 2011 Jul; Prague, Czech Republic; p. 4–7.
7. Xu C, Wang ZZ, Zhang HL, Li HJ, Li DF. Investigation on mode-coupling parametric vibrations and instability of spillway radial gates under hydrodynamic excitation. Appl Math Model. 2022 Feb;106:715–41. doi:10.1016/j.apm.2022.02.013.
8. Zhang B, Jing X. Theoretical analysis and simulation calculation of hydrodynamic pressure pulsation effect and flow-induced vibration response of radial gate structure. Sci Rep. 2022 Dec;12(1):1–13. doi:10.1038/s41598-022-26470-x.
9. Lee SO, Seong H, Kang JW. Flow-induced vibration of a SRG at various opening heights. Eng Appl Comput Fluid Mech. 2018 Jun;12(1):567–83. doi:10.1080/19942060.2018.1479662.
10. Lian JJ, Chen L, Ma B, Liang C. Analysis of the cause and mechanism of hydraulic gate vibration during flood discharging from the perspective of structural dynamics. Appl Sci. 2020 Jan;10(2):629. doi:10.3390/app10020629.
11. Li S, Pan JW, Luo GH, Wang JT. Automatic modal parameter identification of high arch dams: feasibility verification. Earthq Eng Eng Vib. 2020 Oct;19(4):953–65. doi:10.1007/s11803-020-0606-6.
12. Wang G, Li HK, Fu ZY, Huang W, Liu B, Yao SY. A novel methodology for modal parameter identification of arch dam based on multi-level information fusion. Mech Syst Signal Process. 2023 Jan;183(48):109578. doi:10.1016/j.ymssp.2022.109578.
13. Liu B, Li HK, Wang G, Huang W, Wu PZ, Li YK. Dynamic material parameter inversion of high arch dam under discharge excitation based on the modal parameters and Bayesian optimised deep learning. Adv Eng Inform. 2023 Apr;56(2):1–18. doi:10.1016/j.aei.2023.102016.
14. Mostafaei H, Ghamami M, Aghabozorgi P. Modal identification of concrete arch dam by fully automated operational modal identification. Structures. 2021 Aug;32(7):228–36. doi:10.1016/j.istruc.2021.03.028.
15. Zhang YQ, Zhao HD, Fu CJ, Tie Y, Li HL. Automatic identification of the operational modal parameters for hydraulic gates under flow release excitation. Trans Chin Soc Agric Eng. 2022 Oct;38(20):59–66. doi:10.11975/j.issn.1002-6819.2022.20.007.
16. Hu MS, Yang ZZ, Xu J, Zhang B. Modal parameter identification of SRG based on stochastic subspace method. Water Resour Power. 2015 Nov;33(11):164–7.
17. Cai YQ, Zhang K. Study of modal parameter identification from ambient vibration on a deep SRG. Appl Mech Mater. 2011;105–107:511–7. doi:10.4028/www.scientific.net/AMM.105-107.511.
18. Lian JJ, Li HK, Zhang JW. ERA modal identification method for hydraulic structures based on order determination and noise reduction of singular entropy. Sci China Series E: Technol Sci. 2008 Oct;52(2):400–12. doi:10.1007/s11431-008-0200-z.
19. Lu YG, Wan Y. PHA: a fast potential-based hierarchical agglomerative clustering method. Pattern Recognit. 2013 May;46(5):1227–39. doi:10.1016/j.patcog.2012.11.017.
20. Magalhães F, Cunha Á, Caetano E. Online automatic identification of the modal parameters of a long span arch bridge. Mech Syst Signal Process. 2009 Feb;23(2):316–29. doi:10.1016/j.ymssp.2008.05.003.
21. Li HK, Wang G, Wei BW, Li HJ, Li DF. Improved variational mode decomposition method for vibration signal processing of flood discharge structure. J Vib Control. 2022 Oct;28(19–20):2556–2569. doi:10.1177/10775463211016132.

22. Li B, Liang W, Yang S, Zhang L. Automatic identification of modal parameters for high arch dams based on SSI incorporating SSA and K-means algorithm. Appl Soft Comput. 2023 May;138. doi:10.1016/j.asoc.2023.110201.
23. Zhang JW, Hou G, Wang H, Zhao Y, Huang J. Operation feature extraction of flood discharge structure based on improved variational mode decomposition and variance dedication rate. J Vib Control. 2020 Feb;26(3–4):229–40. doi:10.1177/1077546319878542.
24. Li XJ, Li P, Chu FL. Data fusion of multi-sensor vibration signal using correlation function. J Vib Measure Diagn. Jun 2009;29(2):179–183+242. doi:10.16450/j.cnki.issn.1004-6801.2009.02.006.
25. Zhang JW, Hou G, Cao KL, Ma B. Operation conditions monitoring of flood discharge structure based on variance dedication rate and permutation entropy. Nonlinear Dyn. 2018 Sep;93(4):2517–31. doi:10.1007/s11071-018-4339-2.
26. Zhang XC, Lou SY, Chen LY, Wang ZZ, Zhang FF. Study on analysis principle of spatial system method for a hydraulic steel gate. Sustainability. 2022 Nov;14(22):14804. doi:10.3390/su142214804.
27. Buldgen L, Caprace JD, Rigo P, Le Sourne H. Investigation of the added mass method for seismic design of lock gates. Eng Struct. 2017 Jan;131(2):380–93. doi:10.1016/j.engstruct.2016.10.047.